



ELSEVIER

24 April 1995

PHYSICS LETTERS A

Physics Letters A 200 (1995) 299–307

Near-integrability and chaos in a resonant-cavity laser model

Darryl D. Holm^a, Gregor Kovačič^b, Thomas A. Wettergren^b

^a *Theoretical Division, Los Alamos National Laboratory, Los Alamos, NM 87545, USA*

^b *Mathematical Sciences Department, Rensselaer Polytechnic Institute, Troy, NY 12180, USA*

Received 18 August 1994; accepted for publication 1 February 1995

Communicated by C.R. Doering

Abstract

The dynamics of an ensemble of two-level atoms in a single-mode resonant laser cavity with external pumping and a weak coherent probe are investigated. Homoclinic orbits connected to the completely inverted atomic state are found analytically using linear perturbation theory (the Melnikov method) in the near-integrable limit, and are continued in the parameter space to $O(1)$ parameter values using the bifurcation code AUTO. The breakup of these homoclinic orbits is believed to be a source of chaos in the system.

1. Introduction

We describe surfaces of homoclinic orbits in the parameter space of an ensemble of two-level atoms in a single-mode resonant laser cavity with external pumping and a weak coherent probe laser. We assume that the sample of lasing material in the cavity is small enough that we can neglect all spatial effects. The time evolution of the complex envelopes of the electric field \mathcal{E} and the medium polarizability \mathcal{P} , as well as the real-valued population inversion \mathcal{D} , is described by the Maxwell–Bloch equations [1–5],

$$\dot{\mathcal{E}} = \mathcal{P} - \varepsilon\alpha\mathcal{E}, \quad (1a)$$

$$\dot{\mathcal{P}} = (\mathcal{E} + \varepsilon\delta e^{i\omega t})\mathcal{D} - \varepsilon\beta\mathcal{P}, \quad (1b)$$

$$\dot{\mathcal{D}} = -\frac{1}{2}[(\mathcal{E} + \varepsilon\delta e^{i\omega t})\mathcal{P}^* + (\mathcal{E}^* + \varepsilon\delta e^{-i\omega t})\mathcal{P}] - \varepsilon\gamma(\mathcal{D} - 1), \quad (1c)$$

where the overdot denotes the time derivative. All the variables and parameters are dimensionless, their dimensional counterparts and the physical approxima-

tions that go into the derivation of these equations are discussed in Ref. [5] and references therein. The parameter $\varepsilon\alpha$ represents the cavity losses, while $\varepsilon\beta$ and $\varepsilon\gamma$ are the parallel and perpendicular relaxation rates for the lasing material in the cavity, $\varepsilon\delta$ is the strength of the probe laser, and ω is the detuning between the frequencies of the probe light and the radiation in the resonant cavity, which is tuned to match the atomic transition frequency.

2. The integrable limit

In the limit as ε goes to zero in Eqs. (1), we recover the integrable Hamiltonian equations of the classical Jaynes–Cummings model [6]. This integrable limit corresponds to absence of the probe and neglect of both cavity losses and relaxation in the medium. The Jaynes–Cummings equations possess three conserved quantities: unitarity

$$H = \frac{1}{2}|\mathcal{P}|^2 + \frac{1}{2}\mathcal{D}^2,$$

the interaction energy

$$J = (\mathcal{E}\mathcal{P}^* - \mathcal{E}^*\mathcal{P})/2i,$$

and the sum of the field energy and the excitation energy

$$K = \frac{1}{2}|\mathcal{E}|^2 + \mathcal{D}.$$

Eliminating the population inversion \mathcal{D} in favor of the energy K in Eqs. (1) with $\varepsilon = 0$ yields the ideal complex Duffing system,

$$\dot{\mathcal{E}} = \mathcal{P}, \quad \dot{\mathcal{P}} = \mathcal{E}(K - \frac{1}{2}|\mathcal{E}|^2). \quad (2)$$

This system has an important equilibrium at $\mathcal{E} = 0 = \mathcal{P}$. This equilibrium corresponds to the absence of any cavity radiation and material polarizability, with all of the atoms of the material sample being either in the ground state, when $K < 0$, or in the completely inverted state, when $K > 0$. (Polarizability vanishes in these states, because there is no charge separation to form an atomic dipole moment.) The curve of completely-inverted-state equilibria at $\mathcal{E} = 0 = \mathcal{P}$, $K > 0$ is connected to itself by a parametrized family of two-dimensional homoclinic tori, given by the solutions [7,8],

$$\begin{aligned} \mathcal{E} &= 2\sqrt{K} \operatorname{sech}(\sqrt{K} t) e^{i\theta}, \\ \mathcal{P} &= -2K \operatorname{sech}(\sqrt{K} t) \tanh(\sqrt{K} t) e^{i\theta}, \end{aligned} \quad (3)$$

where θ is a time-independent phase angle. This family of homoclinic tori is represented implicitly by the equations,

$$H - \frac{1}{2}K^2 = 0, \quad J = 0. \quad (4)$$

Each torus describes the locus of states undergone by the system as the material emits light into the cavity and reabsorbs it in infinite time. The aim of this paper is to use this family of homoclinic tori as a framework in which to analyze the chaotic behavior of Eqs. (1).

3. The cavity without the probe

In the absence of the probe laser, that is when $\delta = 0$, Eqs. (1) possess a circular symmetry, and therefore contain a continuous family of real subsystems,

$$\dot{\mathcal{E}} = \mathcal{P} - \varepsilon\alpha\mathcal{E}, \quad \dot{\mathcal{P}} = \mathcal{E}(K - \frac{1}{2}\mathcal{E}^2) - \varepsilon\beta\mathcal{P},$$

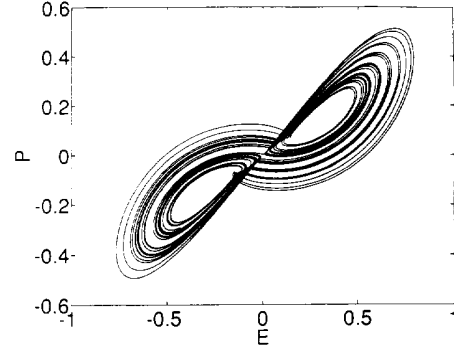


Fig. 1. \mathcal{E} - \mathcal{P} projection of the Lorenz attractor at $(\varepsilon\alpha, \varepsilon\beta, \varepsilon\gamma) = (0.5, 0.1, 0.05)$.

$$\dot{K} = -\varepsilon\alpha\mathcal{E}^2 - \varepsilon\gamma(K - \frac{1}{2}\mathcal{E}^2 - 1), \quad (5)$$

which are obtained by substituting K for \mathcal{D} , writing $\mathcal{E} e^{i\phi}$ and $\mathcal{P} e^{i\phi}$ with real \mathcal{E} and \mathcal{P} instead of the usual complex \mathcal{E} and \mathcal{P} , and noticing that $\dot{\phi} = 0$. This continuous family of real subsystems is precisely the subspace of the complex \mathcal{E} - \mathcal{P} - \mathcal{D} phase space in which $J = 0$. Eqs. (1) with $\delta = 0$ imply $\dot{J} = -\varepsilon(\alpha + \beta)J$, so the $J = 0$ subspace is attracting, and therefore is the only submanifold of importance in the long-time behavior of the system [9].

Haken [10] shows that the real system (5) transforms into the well-known Lorenz equations under the change of variables,

$$\begin{aligned} t &\rightarrow \frac{\sigma}{\varepsilon\alpha}\tau, \quad \mathcal{E} \rightarrow \frac{\varepsilon\alpha}{\sigma}X, \quad \mathcal{P} \rightarrow \frac{\varepsilon^2\alpha^2}{\sigma}Y, \\ \mathcal{D} &\rightarrow \frac{\varepsilon^2\alpha^2}{\sigma}(\rho - Z), \end{aligned}$$

with new parameters b, σ, ρ defined by

$$\sigma = \frac{\alpha}{\beta}, \quad b = \frac{\gamma}{\beta}, \quad \rho = \frac{1}{\alpha\beta\varepsilon^2}.$$

Laser experiments by Arecchi [11] and Weiss et al. [12,13] based on approximations corresponding to system (5) have verified the Lorenz attractor description of single-mode laser dynamics in some parameter regimes. In fact, the Lorenz attractor in the phase space of Eqs. (5) is located in a region of the parameter space near $(\varepsilon\alpha, \varepsilon\beta, \varepsilon\gamma) = (0.5, 0.1, 0.05)$, see Fig. 1. From this viewpoint, the $\varepsilon = 0$ limit of Eqs. (5) is a singular limit of the Lorenz equations as the Rayleigh number ρ goes to infinity [14–16].

The $\varepsilon = 0$ limit of the real system (5) possesses a pair of two-dimensional homoclinic surfaces connecting the curve of completely-inverted-state equilibria to itself. These surfaces are given explicitly by the solutions (3) with $\theta = 0$ and $\theta = \pi$, or implicitly by the first equation in (4), which can be written as

$$\mathcal{P}^2 - K\varepsilon^2 + \frac{1}{4}\varepsilon^4 = 0. \tag{6}$$

For $\varepsilon > 0$, the line $\mathcal{E} = 0 = \mathcal{P}$ is still invariant, and consists of two orbits that contract exponentially towards the only surviving completely-inverted-state equilibrium on it at $\mathcal{E} = 0 = \mathcal{P}$, $K = 1$. This equilibrium is a saddle with a two-dimensional stable and a one-dimensional unstable manifold when $\varepsilon^2\alpha\beta < 1$, and becomes a sink when $\varepsilon^2\alpha\beta > 1$. We seek orbits homoclinic to this completely-inverted-state equilibrium, because they are expected to be a source of chaos in the laser system.

For small values of ε we calculate the parameter regime in which there exist orbits homoclinic to the surviving completely-inverted-state equilibrium by using perturbation theory, that is, by using the Melnikov method [17]. Taking into account the reflection symmetry of the system (5) under $(\mathcal{E}, \mathcal{P}) \mapsto (-\mathcal{E}, -\mathcal{P})$, this method implies that a pair of such homoclinic orbits exists when the Melnikov function, calculated along their unperturbed counterparts, passes through a transverse zero in the $\varepsilon\alpha$ - $\varepsilon\beta$ - $\varepsilon\gamma$ parameter space. This Melnikov function is

$$M(\alpha, \beta, \gamma) = \int_{-\infty}^{\infty} (\mathbf{n} \cdot \mathbf{g})(t) dt,$$

where \mathbf{n} is the gradient of the implicit equation (6) in the \mathcal{E} - \mathcal{P} - K space, and \mathbf{g} is the $O(\varepsilon)$ part of the vector field (5). The integral is calculated along the solutions (3) with $\theta = 0$ and $\theta = \pi$, and $K = 1$. The final result is $M(\alpha, \beta, \gamma) = \frac{8}{3}(3\alpha - \beta - 2\gamma)$ for both orbits. Therefore, a pair of orbits homoclinic to the surviving completely-inverted-state equilibrium exists on a two-dimensional surface in the three-dimensional $\varepsilon\alpha$ - $\varepsilon\beta$ - $\varepsilon\gamma$ parameter space for small $\varepsilon > 0$ near the surface $3\alpha - \beta - 2\gamma = 0$. A similar result appears in Ref. [18].

We continue these homoclinic orbits numerically in the $\varepsilon\alpha$ - $\varepsilon\beta$ - $\varepsilon\gamma$ parameter space by using the code AUTO [19]. We fix $\varepsilon\gamma$ and vary $\varepsilon\alpha$ and $\varepsilon\beta$. Strictly

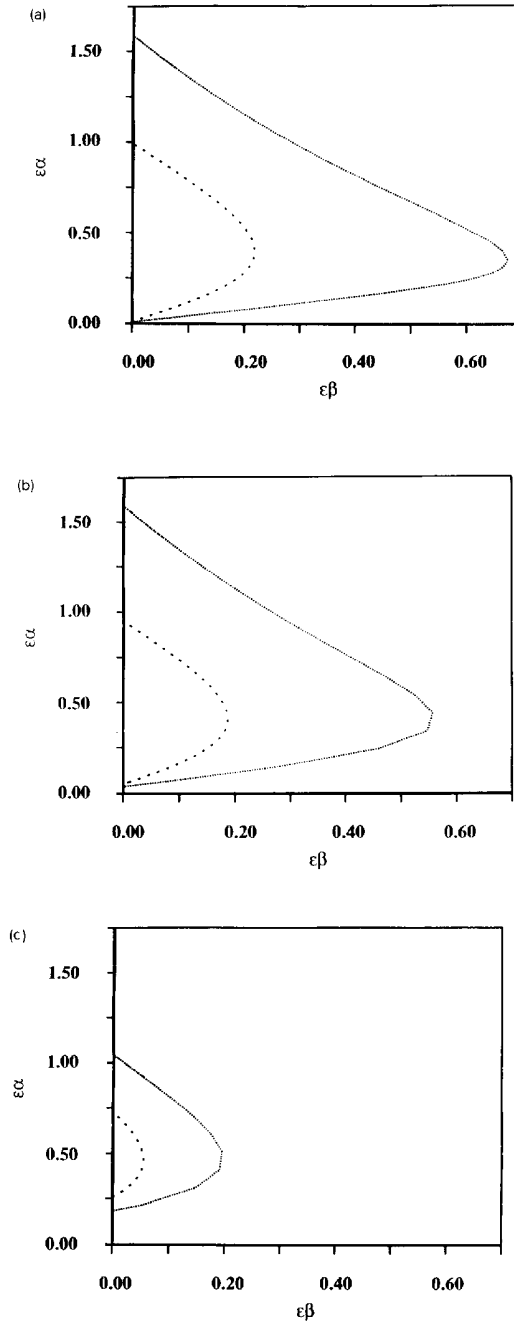


Fig. 2. Locus of points in the $\varepsilon\alpha$ - $\varepsilon\beta$ plane where there exist orbits homoclinic to the completely-inverted-state of the three-dimensional model at fixed values of $\varepsilon\gamma$: (a) $\varepsilon\gamma = 0.01$, (b) $\varepsilon\gamma = 0.05$, (c) $\varepsilon\gamma = 0.226$.

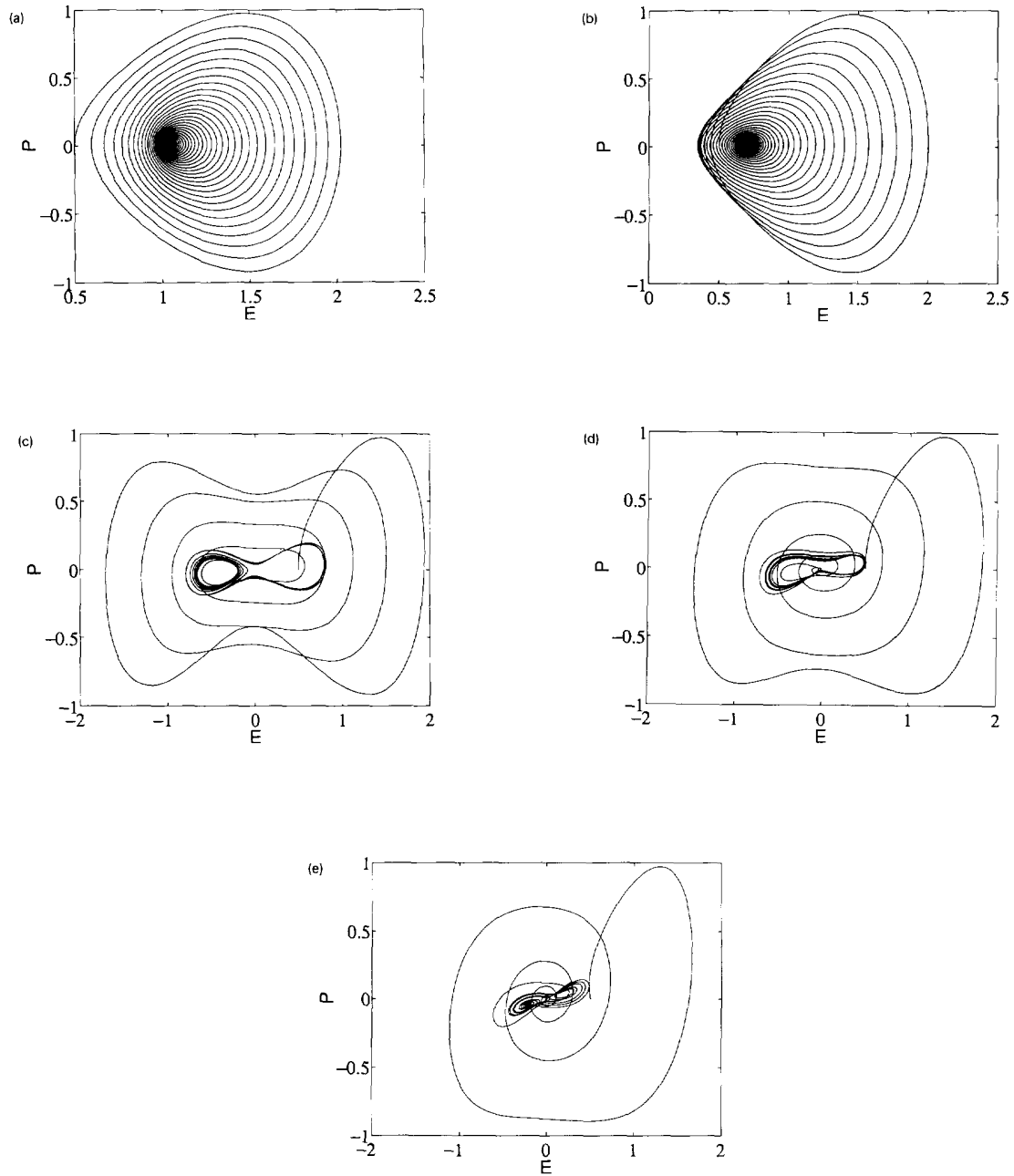


Fig. 3. Bifurcation sequence as $\epsilon\alpha$ increases for fixed $\epsilon\beta = 0.04$ and $\epsilon\gamma = 0.01$ in the three-dimensional model. The trajectories are two-dimensional projections of the true trajectories: (a) $\epsilon\alpha = 0.01$, (b) $\epsilon\alpha = 0.02$, (c) $\epsilon\alpha = 0.05$, (d) $\epsilon\alpha = 0.1$, (e) $\epsilon\alpha = 0.2$.

speaking, we continue periodic orbits of high period (about 500) that are a good approximation to the completely-inverted-state homoclinic orbits. The bottom parts of the curves in the $\varepsilon\alpha$ - $\varepsilon\beta$ plane shown in Fig. 2 on which completely-inverted-state homoclinic orbits exist are very well approximated by the straight lines $3\alpha - \beta - 2\gamma = 0$, as predicted by the Melnikov function, even quite far into the regime of moderate values of the parameters $\varepsilon\alpha$, $\varepsilon\beta$, and $\varepsilon\gamma$. For higher $O(1)$ parameter values, the Melnikov theory does not hold and homoclinic orbits can only be found through numerical procedures.

Chaotic dynamics exist in the neighborhood of this curve where the homoclinic orbits break, which can be seen by constructing a Smale horseshoe map (a standard demonstration for this system is given in Ref. [17]). When the parameters are close to the curve of homoclinic values, the chaotic dynamics cannot be observed due to the presence of spiral sinks. However, these stable equilibrium points undergo a Hopf bifurcation and become unstable as we cross the dashed line in Fig. 2. Inside this region, either the chaotic dynamics may be observed as a strange attractor, or stable limit cycles may be observed (when they exist). In Fig. 2c we see that the homoclinic orbits obtained by numerical continuation of those found with the Melnikov method are consistent with the numerically determined homoclinic orbit found in the Lorenz equations [20] at the parameter values $(\varepsilon\alpha, \varepsilon\beta, \varepsilon\gamma) = (0.847, 0.085, 0.226)$. The existence of these latter homoclinic orbits for nearby parameter values has been shown rigorously in Refs. [21–23] by precise shooting methods. Note that these parameter values are not in the linear region of small parameter values which we were able to predict analytically with the Melnikov method; however, numerical continuation shows that this is precisely the *same* homoclinic orbit as that found with the Melnikov method.

Our study thus yields a fairly complete picture of the two-dimensional surface in the $\varepsilon\alpha$ - $\varepsilon\beta$ - $\varepsilon\gamma$ parameter space on which orbits homoclinic to the completely-inverted-state equilibrium exist. All previously observed homoclinic orbits of the same type lie on this surface [18,20–23]. This surface encloses the smaller surface on which Hopf bifurcations of equilibria take place, and inside which the Lorenz attractor may be observed.

Theoretical and experimental bifurcation sequences have been observed that lead to the occurrence of the Lorenz attractor [11–14,20]. The sequence observed in Refs. [14,20] takes place on a segment of the line $\alpha = 10\beta$, $3\gamma = 8\beta$, which pierces the two-dimensional surface in the $\varepsilon\alpha$ - $\varepsilon\beta$ - $\varepsilon\gamma$ parameter space on which orbits homoclinic to the completely-inverted-state equilibrium exist at the point $(\varepsilon\alpha, \varepsilon\beta, \varepsilon\gamma) = (0.847, 0.085, 0.226)$. The sequence observed in Ref. [12,13] takes place on a segment of the line $\gamma = 0.25\beta$, $\alpha = 4.5\beta$, which lies entirely inside this surface. We propose another type of a bifurcation sequence which takes place on any line $\varepsilon\beta = \text{const}$, $\varepsilon\gamma = \text{const}$ in the $\varepsilon\alpha$ - $\varepsilon\beta$ - $\varepsilon\gamma$ parameter space, along which $\varepsilon\alpha$ is increased. In other words, this sequence leaves the material properties of the lasing medium intact, but varies the cavity losses, which should be easy to achieve experimentally. If we take $\varepsilon\beta$ and $\varepsilon\gamma$ sufficiently small in such a sequence, we can claim that the homoclinic orbits that it encounters are well predicted by the Melnikov method. Moreover, the distance in the parameter space between the point where these homoclinic orbits occur and the point where the strange attractor is first observed is small, which supports the claim that the breakup of these orbits influences the formation of the attractor.

In Fig. 3, we observe one such bifurcation sequence. In particular, this figure shows a sequence of the \mathcal{E} - \mathcal{P} projections of phase trajectories for the Maxwell–Bloch system (5) as the parameter $\varepsilon\alpha$ increases at constant $\varepsilon\beta$ and $\varepsilon\gamma$ along a vertical line in the $\varepsilon\alpha$ - $\varepsilon\beta$ plane. The initial phase point is the same in each case. For $\varepsilon\alpha$ small and below the dotted line in Fig. 2a, Fig. 3a shows that the solution approaches a spiral-sink equilibrium. As $\varepsilon\alpha$ increases to match the homoclinic orbit condition $3\alpha - \beta - 2\gamma = 0$, the solution behavior shows little change, see Fig. 3b. At higher values of $\varepsilon\alpha$ the trajectory approaches a limit cycle, see Fig. 3c. Fig. 3d shows that this limit cycle persists as $\varepsilon\alpha$ increases up to the Hopf bifurcation value, the dashed curve in Fig. 2a. Finally as $\varepsilon\alpha$ increases further, the solution tends to the Lorenz attractor whose \mathcal{E} - \mathcal{P} projection is shown in Fig. 3e.

In the full five-dimensional complex \mathcal{E} - \mathcal{P} - K space, there is a whole circle of orbits homoclinic to the surviving completely-inverted-state equilibrium, and also a whole circle of Lorenz attractors.

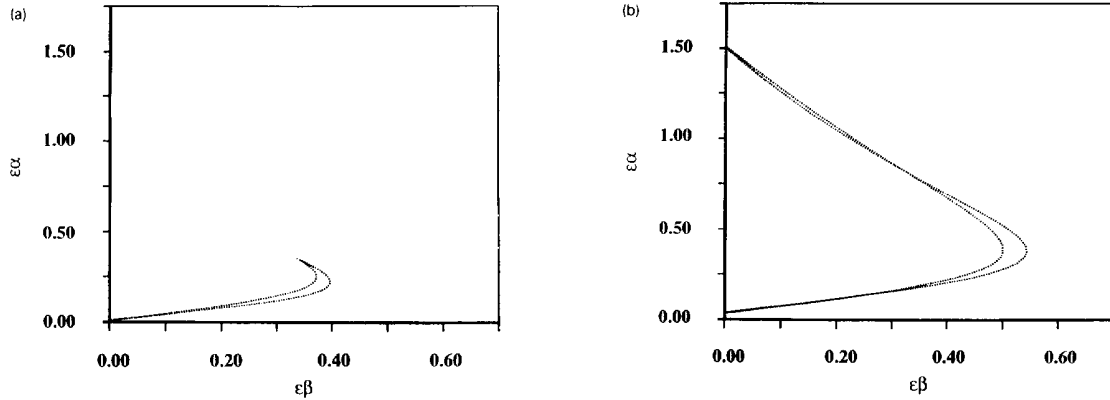


Fig. 4. Locus of points in the $\varepsilon\alpha$ - $\varepsilon\beta$ plane where there exist completely-inverted-state homoclinic orbits of the five-dimensional model at $\varepsilon\delta = 0.1$ and fixed values of $\varepsilon\gamma$: (a) $\varepsilon\gamma = 0.01$, (b) $\varepsilon\gamma = 0.05$.

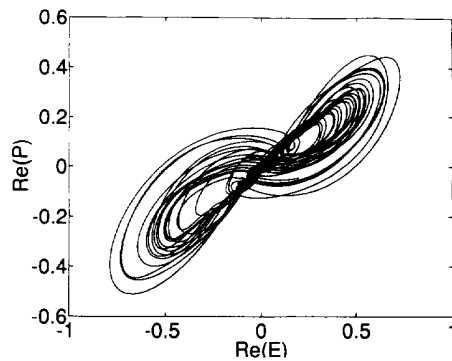


Fig. 5. Two-dimensional projection of the five-dimensional strange attractor caused by orbits homoclinic to the completely-inverted-state at $(\varepsilon\alpha, \varepsilon\beta, \varepsilon\gamma, \varepsilon\delta) = (0.5, 0.1, 0.05, 0.1)$.

4. The cavity with the probe

When the weak laser probe is included in system (1), new variables $E = \mathcal{E} e^{-i\omega t}$, $P = \mathcal{P} e^{-i\omega t}$, $K = \frac{1}{2}|\mathcal{E}|^2 + \mathcal{D}$ may be used to transform this system into the autonomous form

$$\dot{E} = -i\omega E + P - \varepsilon\alpha E, \quad (7a)$$

$$\dot{P} = -i\omega P + (E + \varepsilon\delta)(K - \frac{1}{2}|E|^2) - \varepsilon\beta P, \quad (7b)$$

$$\dot{K} = -\frac{1}{2}\varepsilon\delta(P + P^*) - \varepsilon\alpha|E|^2 - \varepsilon\gamma(K - \frac{1}{2}|E|^2 - 1). \quad (7c)$$

For small enough values of ε , Eqs. (7) have a spiral-saddle completely-inverted-state equilibrium near $E =$

$0 = P$, $K = 1$, with a three-dimensional stable and a two-dimensional unstable manifold. Since the circular symmetry in these equations is broken, we expect to see at most one orbit homoclinic to this equilibrium at any given parameter values. We confirm this by calculating two Melnikov functions,

$$M_j(\alpha, \beta, \gamma) = \int_{-\infty}^{\infty} (\mathbf{n}_j \cdot \mathbf{g})(t) dt, \quad j = 1, 2,$$

where \mathbf{n}_1 and \mathbf{n}_2 are the gradients of the implicit equations (4) in the E - P - K space, and \mathbf{g} is the $O(\varepsilon)$ part of the vector field (7). The integrals are calculated along the orbits (3) transformed into the rotating frame, again with $K = 1$. The results are

$$M_1(\alpha, \beta, \gamma) = \frac{8}{3}(3\alpha - \beta - 2\gamma) + \frac{2}{3}\pi\delta\omega(\omega^2 - 2) \operatorname{sech}(\frac{1}{2}\pi\omega) \sin\theta,$$

$$M_2(\alpha, \beta, \gamma) = -2\pi\delta\omega^2 \operatorname{sech}(\frac{1}{2}\pi\omega) \sin\theta.$$

These functions have simultaneous simple zeros at $\theta = 0$ and $\theta = \pi$, when $3\alpha - \beta - 2\gamma = 0$. Therefore, two families of homoclinic orbits exist on two surfaces that are $O(\varepsilon^2)$ apart from each other and exist near the hyperplane $3\alpha - \beta - 2\gamma = 0$ in the $\varepsilon\alpha$ - $\varepsilon\beta$ - $\varepsilon\gamma$ - $\varepsilon\delta$ parameter space for small enough values of ε .

We again continue these hypersurfaces into larger parameter values by using the code AUTO. We fix $\varepsilon\gamma$ and $\varepsilon\delta$ (and let $\omega = 1$), and continue in $\varepsilon\alpha$ and $\varepsilon\beta$. This continuation confirms that there are two different families of homoclinic orbits, one for $\theta = 0$

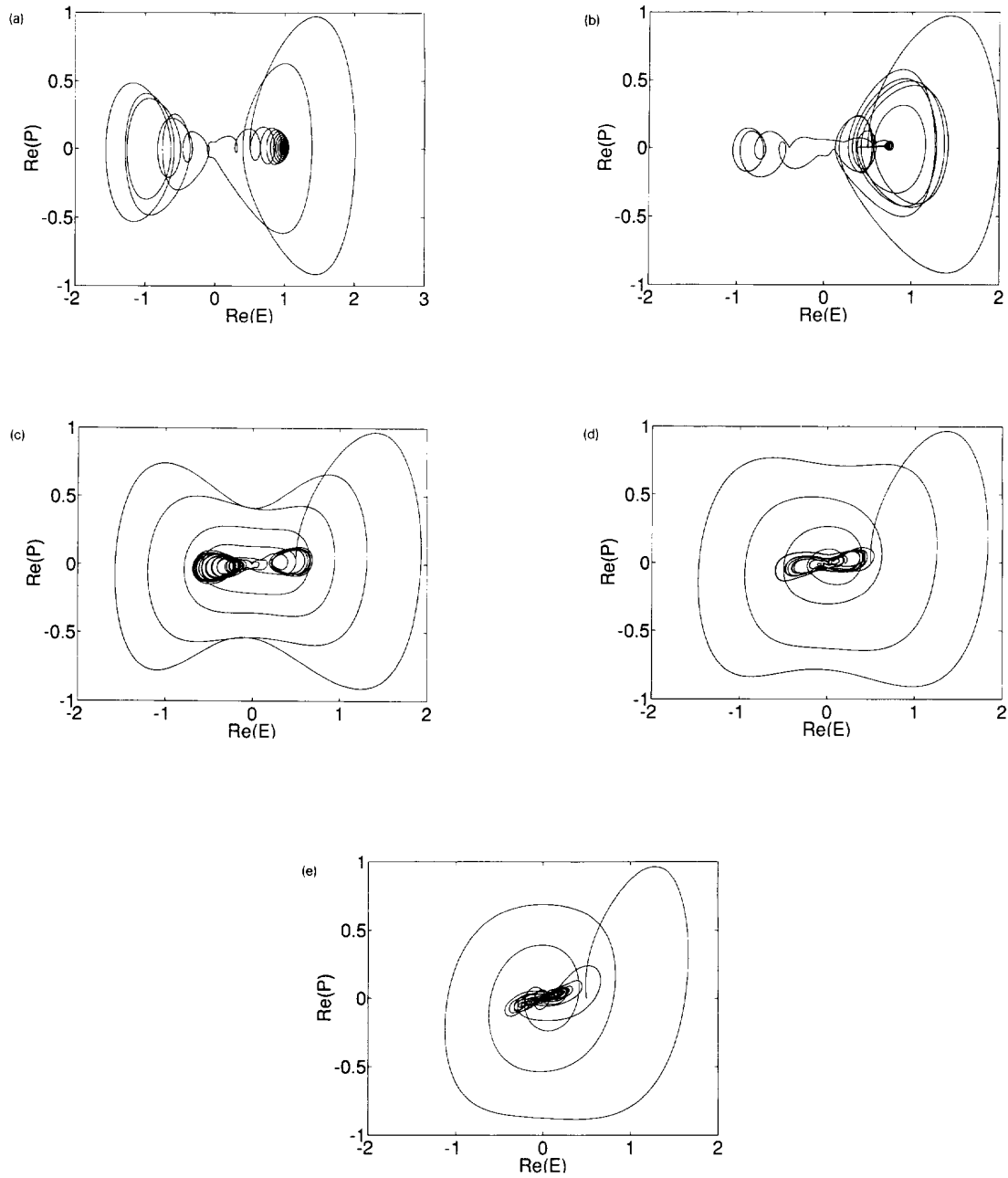


Fig. 6. Bifurcation sequence as $\epsilon\alpha$ increases for fixed $\epsilon\beta = 0.04$, $\epsilon\gamma = 0.01$, and $\epsilon\delta = 0.1$ in the five-dimensional model. The trajectories are two-dimensional projections of the true trajectories: (a) $\epsilon\alpha = 0.01$, (b) $\epsilon\alpha = 0.02$, (c) $\epsilon\alpha = 0.05$, (d) $\epsilon\alpha = 0.1$, (e) $\epsilon\alpha = 0.2$.

and one for $\theta = \pi$, which exist along $\varepsilon\alpha$ - $\varepsilon\beta$ curves that are tangent near $\varepsilon\beta = 0$. As shown in Fig. 4, the $\varepsilon\alpha$ - $\varepsilon\beta$ curves along which orbits homoclinic to the completely-inverted-state equilibrium exist are again well approximated by the equation $3\alpha - \beta - 2\gamma = 0$ implied by the Melnikov method, even well into the region of moderate values of $\varepsilon\alpha$, $\varepsilon\beta$, and $\varepsilon\gamma$. From Fig. 4, it is seen that the parameter region where homoclinic orbits exist with the probe is similar to that without the probe when $\varepsilon\gamma$ and $\varepsilon\delta$ are of the same order of magnitude. As the probe strength is increased and $\varepsilon\delta$ becomes much larger than $\varepsilon\gamma$ we see that the similarity between the probe and no-probe case only holds for small values of $\varepsilon\alpha$ and $\varepsilon\beta$.

The homoclinic orbits found in these continuations are Šilnikov saddle-focus connections [24–27], and they induce chaotic dynamics by the Smale horseshoe mechanism for parameter values in the vicinity of the curves in Fig. 4. A two-dimensional projection of the five-dimensional chaotic attractor is shown in Fig. 5. A bifurcation sequence obtained by fixing the material relaxation parameters $\varepsilon\beta$ and $\varepsilon\gamma$ and the probe strength $\varepsilon\delta$, and increasing the cavity losses $\varepsilon\alpha$ is shown in Fig. 6.

5. Conclusion

We have determined the shape and position of the surfaces in the parameter space of the Maxwell–Bloch equations with and without the probe on which orbits homoclinic to the completely-inverted-state equilibrium exist. These surfaces contain all previously known cases of the same type of homoclinic orbits observed in the phase space of the equations without the probe. These homoclinic orbits are believed to provide much of the structure under which strange attractors develop [14,20], hence their existence is of great interest in the study of chaos. It may be possible to develop experimental methods to observe them, perhaps by designing methods for controlling chaos [28–33] that mimic the AUTO code. These methods would provide a better confirmation of the validity of the mathematical model than do conventional methods such as power spectra or Lyapunov exponents, because they would identify the homoclinic orbits directly, instead of by inference from their effects.

Acknowledgement

We thank Charlie Doering and Ben Luce for helpful advice. G.K. and T.A.W. would like to thank the Theoretical Division and the Center for Nonlinear Studies at the Los Alamos National Laboratory for their hospitality and support during the Summers of 1992, 1993, and 1994. D.D.H. was supported by DOE contract number W-7405-Eng-36 and Office of Basic Energy Science, Department of Applied Mathematics. G.K. and T.A.W. were supported by the U.S. Department of Energy grant DE-FG02-93ER25154, and by the National Science Foundation grant DMS-9403750.

References

- [1] L. Allen and J.H. Eberly, *Optical resonance and two-level atoms* (Dover, New York, 1987).
- [2] K.N. Alekseev and G.P. Berman, *Sov. Phys. JETP* 65 (1987) 1115.
- [3] Special issue on Nonlinear dynamics of lasers, *J. Opt. Soc. B* 5 (1988).
- [4] J.V. Moloney and A.C. Newell, *Physica D* 44 (1990) 1.
- [5] D.D. Holm and G. Kovačič, *Physica D* 56 (1992) 270.
- [6] E.T. Jaynes and F.N. Cummings, *Proc. IEEE* 51 (1963) 89.
- [7] D.D. Holm, G. Kovačič and B. Sundaram, *Phys. Lett. A* 154 (1991) 346.
- [8] D.D. Holm, G. Kovačič and T.A. Wettergren, Homoclinic orbits in the Maxwell–Bloch equations with a probe, preprint (1994).
- [9] L.A. Pokrovskii, *Theor. Math. Phys.* 62 (1986) 183.
- [10] H. Haken, *Phys. Lett. A* 53 (1975) 77.
- [11] F.T. Arecchi, *Acta Phys. Austr.* 56 (1984) 57.
- [12] C.O. Weiss and W. Klische, *Opt. Commun.* 51 (1984) 47.
- [13] C.O. Weiss, N.B. Abraham and U. Hübner, *Phys. Rev. Lett.* 61 (1988) 1587.
- [14] C. Sparrow, *The Lorenz equations* (Springer, Berlin, 1982).
- [15] A.C. Fowler, *Stud. Appl. Math.* 70 (1984) 215.
- [16] L.A. Pokrovskii, *Theor. Math. Phys.* 67 (1986) 490.
- [17] S. Wiggins, *Global bifurcations and chaos: Analytical methods* (Springer, Berlin, 1988).
- [18] J. Li and J. Zhang, *SIAM J. Appl. Math.* 53 (1993) 1059.
- [19] E.J. Doedel and P. Kernévez, AUTO: software for continuation and bifurcation problems in ordinary differential equations, *Applied Mathematics Report*, Caltech (1986).
- [20] J.L. Kaplan and J.A. Yorke, *Commun. Math. Phys.* 67 (1979) 93.
- [21] S.P. Hastings and W.C. Troy, *Bull. Am. Math. Soc.* 27 (1992) 298.
- [22] S.P. Hastings and W.C. Troy, *J. Differ. Eqs.*, to be published.
- [23] B.D. Hassard and J. Zhang, *SIAM J. Math. Anal.* 25 (1994) 179.
- [24] L.P. Šilnikov, *Sov. Math. Dokl.* 6 (1965) 163.
- [25] L.P. Šilnikov, *Sov. Math. Dokl.* 8 (1967) 102.

- [26] L.P. Šilnikov, *Math. USSR Sb.* 10 (1970) 91.
- [27] B. Deng, *J. Differ. Eqs.* 102 (1993) 305.
- [28] E. Ott, C. Grebogi and J.A. Yorke, *Phys. Rev. Lett.* 64 (1990) 1196.
- [29] I.B. Schwartz and I. Triandaf, *Phys. Rev. A* 46 (1992) 7439.
- [30] Z. Gills, C. Iwata, R. Roy, I.B. Schwartz and I. Triandaf, *Phys. Rev. Lett.* 69 (1992) 3169.
- [31] R. Roy, T.W. Murphy Jr., T.D. Maier, Z. Gills and E.R. Hunt, *Phys. Rev. Lett.* 68 (1992) 1259.
- [32] A. Gavrielides and V. Kovanis, *Taming chaos in semiconductor lasers with optical feedback*, preprint (1993).
- [33] T.A. Wettergren, *A control method for tracking homoclinic orbits in a laser system* (1994).